Activation of PPARα Ameliorates Hepatic Insulin Resistance and Steatosis in High Fructose–Fed Mice Despite Increased Endoplasmic Reticulum Stress

Stanley M.H. Chan,[1] Ruo-Qiong Sun,[1] Xiao-Yi Zeng,[1] Zi-Heng Choong,[1] Hao Wang,[1] Matthew J. Watt,[2] and Ji-Ming Ye[1]

Endoplasmic reticulum (ER) stress is suggested to cause hepatic insulin resistance by increasing de novo lipogenesis (DNL) and directly interfering with insulin signaling through the activation of the c-Jun N-terminal kinase (JNK) and IκB kinase (IKK) pathway. The current study interrogated these two proposed mechanisms in a mouse model of hepatic insulin resistance induced by a high fructose (HFru) diet with the treatment of fenofibrate (FB) 100 mg/kg/day, a peroxisome proliferator–activated receptor α (PPARα) agonist known to reduce lipid accumulation while maintaining elevated DNL in the liver. FB administration completely corrected HFru-induced glucose intolerance, hepatic steatosis, and the impaired hepatic insulin signaling (pAkt and pGSK3β). Of note, both the IRE1/XBP1 and PERK/eIF2α arms of unfolded protein response (UPR) signaling were activated. While retaining the elevated DNL (indicated by the upregulation of SREBP1c, ACC, FAS, and SCD1 and [^{3}H]H_2O incorporation into lipids), FB treatment markedly increased fatty acid oxidation (indicated by induction of ACOX1, p-ACC, β-HAD activity, and [^{14}C]palmitate oxidation) and eliminated the accumulation of diacylglycerols (DAGs), which is known to have an impact on insulin signaling. Despite the marked activation of UPR signaling, neither JNK nor IKK appeared to be activated. These findings suggest that lipid accumulation (mainly DAGs), rather than the activation of JNK or IKK, is pivotal for ER stress to cause hepatic insulin resistance. Therefore, by reducing the accumulation of deleterious lipids, activation of PPARα can ameliorate hepatic insulin resistance against increased ER stress. ***Diabetes*** **62:2095–2105, 2013**

Liver is one of the most metabolically active and insulin responsive organs that regulate glucose homeostasis, lipid metabolism, and protein synthesis (1). Under normal conditions, insulin suppresses hepatic glucose production from glycogenolysis and gluconeogenesis while promoting glucose storage in the form of glycogen to help to control postprandial glucose level. However, the ability of insulin to shut down glucose production from the liver is diminished under a state of hepatic insulin resistance, which in turn leads to the manifestation of hyperglycemia (2). Although the pathogenesis of hepatic insulin resistance is likely to be multifactorial, increased endoplasmic reticulum (ER) stress and an accumulation of lipids within the liver have been demonstrated to be important mechanisms (3,4).

Lipid accumulation in the liver, or hepatic steatosis, can lead to insulin resistance by interfering with insulin signal transduction through lipid metabolites, such as diacylglycerols (DAGs) and ceramide (4). Hepatic steatosis can result from increased fatty acid (FA) influx, elevated de novo lipogenesis (DNL), and reduced FA oxidation (1,4). In humans, elevated DNL from increased consumption of sucrose is the predominant mechanism for the development of hepatic steatosis, with fructose (breakdown product of sucrose) being the major culprit (5,6).

Recent studies in animal models (7,8) identified a possible role of ER stress in the development of hepatic insulin resistance during elevated DNL. When ER stress occurs, the ER mounts the unfolded protein response (UPR), which involves the activation of three major branches of signal transducers: inositol-requiring protein 1 (IRE1), protein kinase RNA-like ER kinase (PERK), and activating transcription factor 6 (ATF6) (9). Activation of these canonical mechanisms is crucial for cellular adaption and resolution of ER stress. However, chronic activation of UPR signaling has been demonstrated to activate c-Jun N-terminal kinase (JNK) and IκB kinase (IKK). The IRE1 branch of the UPR can activate JNK (10) and IKK (11) by forming a complex with the tumor-necrosis factor receptor-associated factor 2. Meanwhile, the PERK/eukaryotic translation initiation factor 2α (eIF2α) branch has also been reported to be capable of activating JNK (12). Because activated JNK (8,13) and IKK (14) can direct serine/threonine phosphorylation of insulin receptor substrate (IRS), leading to the inhibition of insulin signaling transduction, it has been suggested that JNK and IKK are the key molecules linking activated UPR and hepatic insulin resistance (15).

More recently, we found that elevated DNL and insulin resistance in the liver of high fructose (HFru)–fed mice is coupled with activation of the IRE1 and PERK branches of the UPR (16). However, it is unclear whether hepatic insulin resistance results from lipid accumulation or activated JNK and IKK pathways during increased ER stress. Of interest, hepatic DNL is increased by the activation of peroxisome proliferator–activated receptor α (PPARα) (17,18), which has also been shown to reverse hepatic steatosis (19,20). Because ER stress is tightly associated with DNL, we hypothesized that treatment of HFru-fed mice with a PPARα agonist activates both the IRE1 and the PERK branches while preventing hepatic steatosis. Under these conditions, we would then be able to interrogate the implication of these two mechanisms (lipid accumulation

From the [1]Molecular Pharmacology for Diabetes Group, Health Innovations Research Institute and School of Health Sciences, RMIT University, Melbourne, Victoria, Australia; and the [2]Biology of Lipid Metabolism Laboratory, Department of Physiology, Monash University, Melbourne, Victoria, Australia.

Corresponding author: Ji-Ming Ye, jiming.ye@rmit.edu.au.

Received 8 October 2012 and accepted 11 January 2013.

DOI: 10.2337/db12-1397

This article contains Supplementary Data online at http://diabetes.diabetesjournals.org/lookup/suppl/doi:10.2337/db12-1397/-/DC1.

S.M.H.C. and R.-Q.S. contributed equally to this study.

or activated JNK and IKK) in hepatic insulin resistance in the face of increased ER stress. The results show that accumulation of lipids, namely DAGs, rather than the activation of JNK or IKK is the key factor of hepatic insulin resistance during increased ER stress. Activation of PPARα with fenofibrate (FB) can eliminate hepatic insulin resistance during HFru feeding by reducing DAG levels, despite the presence of ER stress as evidenced by the dual activation of the IRE1/X-box binding protein 1 (XBP1) and PERK/eIF2α pathways.

RESEARCH DESIGN AND METHODS

Animals. Male C57BL/6J mice (aged 14 weeks) from the Animal Resources Centre (Perth, Australia) were kept at 22 ± 1°C on a 12-h light/dark cycle. After 1 week of acclimatization, mice were fed ad libitum for up to 15 days with either a chow (CH) or an HFru diet. The CH diet comprised 70% calories from starch, ~10% calories from fat, and ~20% calories from protein (Specialty Feeds, Glen Forrest, Western Australia), and the HFru diet comprised 35% fructose, 35% starch, ~10% fat, and ~17% protein. The detailed recipe for the HFru diet is described in our previous studies (16,21). FB (Sigma-Aldrich, Castle Hill, New South Wales, Australia) was provided as a supplement by mixing it into the diets at a concentration of 100 mg/kg/day. All experiments were approved by the Animal Ethics Committees of RMIT University (#1012).

Body weight and food intake were measured daily. The whole-body metabolic rate was measured at 22°C using an indirect calorimeter (Comprehensive Laboratory Animal Monitoring System; Columbus Instruments, Columbus, OH) as described previously (22) between 5 and 8 days after the administration of FB. Mice were fasted for 5–7 h before being killed; tissues of interest were collected and freeze-clamped immediately. Epididymal fat mass was weighed using an analytical balance. Liver triglycerides were extracted by the method of Folch and determined by a Peridochrom Triglyceride GPO-PAP kit (Roche Diagnostics Australia) as previously described (16). In separate experiments, glucose tolerance tests (GTTs) (glucose 2.5 g/kg i.p.) were performed on the 5–7-h fasted mice using a glucometer (Accu-Chek Performa Nano; Roche, Victoria, Australia), and blood samples were collected at 0, 30, and 60 min for plasma insulin measurement. For the assessment of insulin signaling in the liver, the mice were injected with insulin 2 U/kg i.p. 20 min before tissue collection.

Measurement of hepatic FA oxidation DNL. FA oxidation was measured in liver homogenates using methods described previously (23). Briefly, the liver homogenate (50 μL) was incubated at 30°C for 90 min in a reaction mixture (pH 7.4) containing (in mmol/L) 0.2 [^{14}C]palmitate (0.5 μCi); 2 L-carnitine; and 0.05 CoA ± 0.02 etomoxir, a specific inhibitor of FA oxidation in mitochondria (24). The reaction was stopped by ice-cold 1 mol/L perchloric acid. CO_2 produced from the reaction was captured in 1 mol/L NaOH. ^{14}C counts in the acid-soluble fraction were combined with the CO_2 values to give the total palmitate oxidation rate. Hepatic DNL was determined by measuring the incorporation of [^{3}H]H_2O into triglyceride (TG) in the liver as described previously (16,25).

Citrate synthase and β3-hydroxyacyl-CoA dehydrogenase activity. Approximately 20 mg of frozen liver tissue was homogenized in 175 mmol/L KCl and 1.98 mmol/L EDTA-containing buffer (pH 7.4) with a glass homogenizer before being subjected to three freeze-thaw cycles. Citrate synthase and β3-hydroxyacyl-CoA dehydrogenase (β-HAD) activities were determined as described previously (16,21) with a Flexstation 3 plate reader (Molecular Devices, Sunnyvale, CA).

Western blotting. Liver and red quadriceps muscle samples were homogenized in ice-cold lysis buffer (pH 7.5) containing (in mmol/L) 50 Tris, 150 NaCl, 1% Triton X-100, 10 NaP, 100 NaF, 2 Na_3VO_4, 1 EDTA, 1 EGTA, and 10% glycerol supplemented with protease inhibitor cocktail and phosphates inhibitor cocktail (Sigma Aldrich) and DL-dithiothreitol. Protein samples were then denatured in SDS sample buffer (125 mmol/L Tris-HCl, pH 6.8, 50% glycerol, 2% SDS, 5% β-mercaptoethanol, and 0.01% bromophenol blue). The insulin signal transduction was assessed by total and phosphorylated (Ser473) Akt and total and phosphorylated (Ser219) glycogen synthase kinase 3β (GSK-3β) (Cell Signaling Technology). Key lipogenic enzymes were determined by Western blotting with specific antibodies, including sterol regulatory element-binding protein (SREBP1c) (Santa Cruz Biotechnology), phosphorylated and total acetyl-CoA carboxylase (ACC) (Cell Signaling), fatty acid synthase (FAS) (Cell Signaling), and stearoyl-CoA desaturase 1 (SCD-1) (Cell Signaling). Oxidative capacity included acyl-CoA oxidase 1 (ACOX1) (Santa Cruz). ER stress included phosphorylated (Thr980) PERK (p-PERK) (Cell Signaling), total and phosphorylated (Ser51) eIF2α (Cell Signaling), growth arrest and DNA damage-inducible protein 34 (GADD34) (Cell Signaling), CCAAT/enhancer-binding protein (C/EBP) homologous protein (CHOP) (Santa Cruz), phosphorylated (Ser724) IRE1 (Abcam), XBP1 (Santa Cruz), and activating transcription factor 6 α (ATF6α) (Santa Cruz). Serine/threonine kinases included phosphorylated (Ser176/177) IKKα/IKKβ (Cell Signaling), IκBα, and phosphorylated (Thr183/Tyr185) JNK (Cell Signaling). Immunolabeled bands were quantified by densitometry, and representative blots are shown.

Analyses of hepatic lipids. DAG and ceramide were extracted and quantified according to the methods of Preiss et al. (26). Lipids were extracted from liver homogenates using chloroform:methanol:PBS + 0.2% SDS (1:2:0.8). DAG kinase and ^{32}P-labeled ATP (0.55 GBq/mmol cold ATP) were added to the lysates preincubated with cardiolipin/octylglucoside, and the reaction was stopped after 2.5 h by the addition of chloroform:methanol (2:1). Samples were spotted onto thin-layer chromatography plates and developed. ^{32}P-labeled phosphatidic acid and ceramide-1-phosphate were identified by autoradiography, dried, scraped from the thin-layer chromatography plate, and counted in a liquid scintillation analyzer (LS6500; Beckman Coulter Inc.).

Statistical analysis. Data are presented as mean ± SE. One-way ANOVA was used for comparison of the relevant groups. When significant differences were found, the Turkey-Kramer multiple comparisons test was applied. Differences at $P < 0.05$ were considered to be statistically significant.

RESULTS

FB treatment normalizes HFru feeding–induced adiposity and improved glucose intolerance. HFru feeding resulted in significant increases in calorie intake (~38%), whole-body V_{O_2} (~8%) and respiratory exchange ratio (RER), body weight gain (1.2 g), and adiposity (67% in epididymal fat mass, $P < 0.01$) compared with untreated CH-fed mice (CH-Veh) (Table 1). In CH-fed mice, FB treatment had no significant effects on body weight gain, adiposity, caloric intake, or RER except for a 14% increase in V_{O_2} ($P < 0.05$ vs. CH-Veh). In HFru-fed mice, FB significantly ($P < 0.05$ for all) increased V_{O_2} (8%), reduced the RER, and completely diminished HFru-induced body weight gain and adiposity. FB lowered blood glucose and insulin levels in the HFru-fed mice (both $P < 0.01$ HFru-FB) and, hence, led to an improved homeostasis model assessment insulin resistance (HOMA-IR) index. The untreated HFru-fed mice (HFru-Veh) showed glucose intolerance compared with CH-Veh (Fig. 1*A* and *B*). FB treatment completely normalized the glucose tolerance seen in the HFru-fed mice to the levels of the CH-fed mice and reduced the requirement for plasma insulin level (Fig. 1*C*).

FB treatment restored hepatic insulin signal transduction in HFru-fed mice. In skeletal muscle, the insulin-stimulated phosphorylation of Akt (all $P < 0.001$ vs. corresponding basal) was unaltered by diet or FB treatment (Supplementary Fig. 1). In contrast, HFru feeding blunted the insulin-stimulated phosphorylation of Akt (by 53%, $P < 0.01$ vs. CH) and its downstream target GSK3β (by 60%, $P < 0.001$ vs. CH) in the liver, which were fully restored by the treatment of FB (Fig. 2*A* and *B*), indicating that HFru feeding results in impairment of hepatic insulin signaling and that treatment with FB is effective in restoring hepatic insulin sensitivity.

FB treatment normalized hepatic lipid accumulation. Lipid accumulation in the liver (i.e., hepatic steatosis) is believed to be closely linked to insulin resistance (1); hence, we examined the effects of FB treatment on hepatic lipid content. As expected, the HFru feeding induced a marked increase in hepatic TG levels (2.7-fold, $P < 0.01$ vs. CH), which was ameliorated by treatment with FB (Fig. 3*A*), although the fasting plasma TG levels were unaffected between the HFru-Veh and HFru-FB groups (Table 1). In agreement with an increased TG level, hepatic DAG content of the HFru-fed mice was also elevated by 53% ($P < 0.05$ vs. CH), which was normalized by treatment with FB (Fig. 3*B*). The total content of ceramide was attenuated by 57% ($P < 0.001$ vs. CH) by HFru feeding

TABLE 1
Basal metabolic parameters of HFru-fed mice

	CH-Veh	CH-FB	HFru-Veh	HFru-FB
Body mass (g)				
Day 0	27.0 ± 0.4	27.5 ± 0.4	28.0 ± 0.5	26.8 ± 0.4
Day 14	28.0 ± 0.4	27.9 ± 0.4	29.2 ± 0.4[a]	22.2 ± 0.6[b,d,e]
EPI/BW	1.2 ± 0.1	1.0 ± 0.1	2.0 ± 0.3[b]	0.7 ± 0.1[a,d]
Caloric intake (kcal/kg/day)	411 ± 6.6	436 ± 12.3	571 ± 9.7[b,e]	567 ± 13.6[b,e]
VO_2 (L/kg/h)	3.23 ± 0.07	3.70 ± 0.14[a]	3.50 ± 0.03[a]	3.78 ± 0.13[a,c]
RER	0.93 ± 0.01	0.92 ± 0.01	0.97 ± 0.01[a]	0.93 ± 0.02[c]
Blood glucose (mmol/L)	8.4 ± 0.3	10.5 ± 0.4[a]	10.2 ± 0.5[a]	6.6 ± 0.4[a,d,e]
Plasma insulin (pg/mL)	203 ± 23	91 ± 16[b]	208 ± 26[e]	82 ± 6[b,d]
HOMA-IR	77.4 ± 9.0	40.9 ± 6.7[a]	96.3 ± 16.8[e]	23.3 ± 2.2[b,d,e]
Plasma TG (μmol/L)	354 ± 20	176 ± 10[b]	264 ± 16[b,e]	260 ± 32[b,e]

Data are mean ± SE, 8–12 mice per group. Male C57BL/6J male mice were fed either a CH or HFru diet for 2 weeks with or without the supplementation of a PPARα agonist, FB 100 mg/kg/day. The data for whole-body VO_2 and RER were the average values of 24 h of measurement after 1 week of FB administration. HOMA-IR was calculated as follows: [fasting blood glucose (mmol/L) × fasting insulin (mU/L)]/22.5. [a]$P < 0.05$; [b]$P < 0.01$ vs. CH-Veh. [c]$P < 0.05$; [d]$P < 0.01$ vs. HFru-Veh. [e]$P < 0.01$ vs. CH-FB.

but was restored (P n.s. vs. CH-Veh and CH-FB) by treatment with FB (Fig. 3*C*). These data suggest that the implication of DAG in the apparent hepatic insulin resistance resulted from HFru feeding.

FB treatment increases hepatic fat oxidation under HFru feeding conditions. Because enhanced FA oxidation is one of the key events resulting from the activation of PPARα by FB in the liver (27–29), we measured molecular markers of oxidative capacity in the livers of mice. The expression of peroxisomal ACOX1, a direct downstream effector of PPARα activation that catalyses the first step of peroxisomal β-oxidation of FAs (30), was markedly upregulated in response to treatment with FB (Fig. 4*A*). Moreover, the phosphorylation of ACC, which regulates

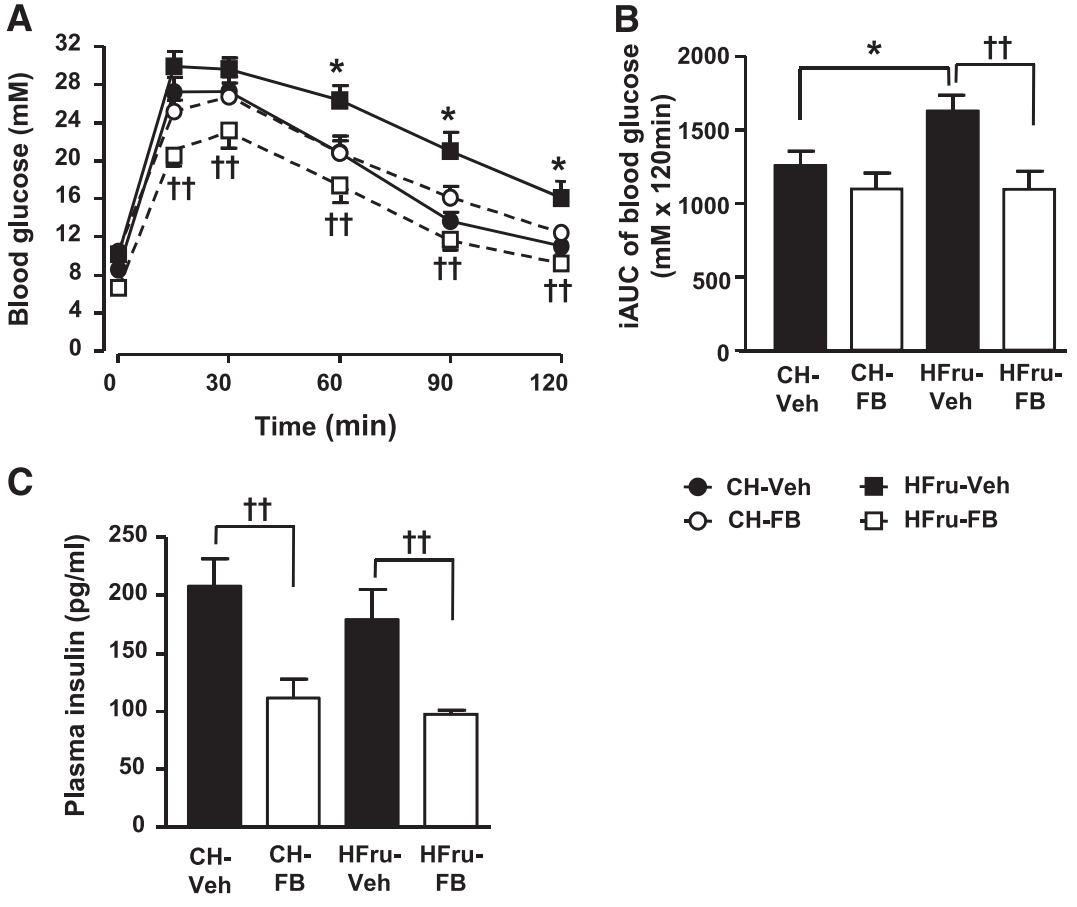

FIG. 1. Effects of FB treatment on glucose tolerance. Male C57BL/6J mice were fed an HFru diet with or without the supplementation of FB 100 mg/kg/day compared with a standard laboratory CH diet. The experiments were performed after 2 weeks of CH, CH-FB, HFru, or HFru-FB feeding. *A*: GTT was performed with an injection of glucose 2.5 g/kg i.p. after 5–7 h of fasting. *B*: Incremental area under the curve (iAUC) for blood glucose level. *C*: Plasma insulin level between 30–60 min of GTT. Data are mean ± SE, 8–12 mice per group. *$P < 0.05$; ††$P < 0.01$ of the compared groups.

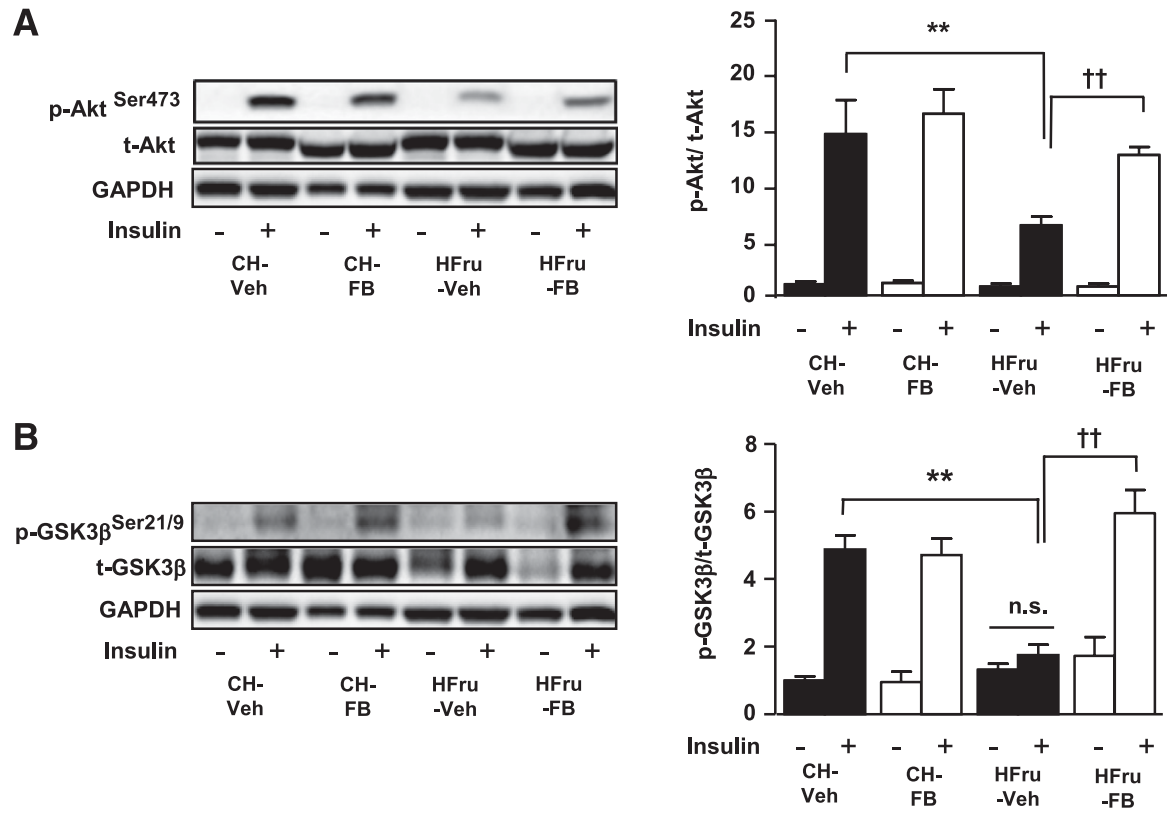

FIG. 2. Effects of FB treatment on hepatic insulin signal transduction. After 2 weeks of feeding, animals were fasted for 5–7 h before tissue collection, and liver homogenates were prepared for immunoblotting. *A*: Representative blots of phosphorylated (p) and total (t) Akt (Ser473) with densitometry in the liver. *B*: Representative blots of p- and t-GSK3β (Ser21/9) with densitometry in the liver in response to a bolus of insulin stimulation of 2 U/kg i.p. Each lane represents a single mouse. Data are mean ± SE, 8 mice per group. All insulin-stimulated groups reached statistical significance of $P < 0.01$ compared with their corresponding basal groups, unless otherwise indicated. **$P < 0.01$; ††$P < 0.001$ of the compared groups.

the mitochondrial β-oxidation of FAs, was markedly elevated (eightfold, $P < 0.001$ vs. CH-Veh and HFru-Veh) in response to FB treatment in the livers of HFru-fed mice (Fig. 4*B*). In line with an increased oxidative capacity, the activity of β-HAD, which catalyses the third step of mitochondrial β-oxidation, was augmented by 2.4-fold ($P < 0.01$ vs. CH-Veh and HFru-Veh) with FB treatment in the HFru-fed mice (Fig. 4*C*). The activity of citrate synthase was significantly enhanced (by 19%, $P < 0.01$ vs. CH) with HFru feeding independently of PPARα activation (Fig. 4*D*), indicating that PPARα activation specifically enhances the oxidative capacity of the liver without affecting mitochondrial content under HFru feeding conditions. Hepatic FA oxidation was increased (~60%) by treatment with FB in the HFru-fed mice, and this resulted in an increase in the component resistant to the inhibition by etomoxir (Fig. 4*E*).

FB treatment triggered the activation of UPR pathways in the liver. Having established that treatment with FB was effective in eliminating hepatic lipid accumulation and restoring insulin signaling, we next examined the effects of FB on the three major UPR pathways. The phosphorylation of IRE1 (Fig. 5*A*), spliced form of XBP1 (sXBP1) (Fig. 5*B*), phosphorylation of PERK and eIF2α (Fig. 5*C* and *D*), and expression of CHOP (Fig. 5*E*) were markedly enhanced by PPARα activation, regardless of the feeding conditions. In addition, the expression of GADD34, a well-characterized phosphatase of eIF2α (9), was concomitantly downregulated in response to PPARα activation (Fig. 5*F*). As expected, HFru feeding significantly increased the phosphorylated form of IRE1 ($P < 0.05$ vs. CH) (Fig. 5*A*) and eIF2α ($P < 0.01$ vs. CH) (Fig. 5*D*). No changes were detected in the maturation of ATF6 as a result of HFru feeding or FB treatment (Supplementary Fig. 2).

FB-induced UPR signaling was accompanied by an enhanced DNL. Because both activation of PPARα (28) and UPR signaling (7) can promote DNL in the liver through the action of SREBP1c (31), we examined the expression of SREBP1c and key enzymes involve in this process. The Western blot analysis revealed upregulations of the mature form of SREBP1c (mSREBP1c) (threefold, $P < 0.05$ vs. CH-Veh), ACC (3.5-fold, $P < 0.01$ vs. CH-Veh), FAS (2.5-fold, $P < 0.001$ vs. CH), and SCD1 (14.5-fold, $P < 0.01$ vs. CH-Veh) in the liver of the HFru-fed mice (Fig. 6*A*–*D*). PPARα activation in the CH-fed mice stimulated the expression of mSREBP1c, ACC, FAS, and SCD1 to levels comparable with that of the HFru-fed mice. PPARα activation in conjunction with HFru feeding elicited a further increase in the expression of mSREBP1c (sixfold) and SCD1 (38-fold, both $P < 0.001$ vs. HFru-Veh) but not ACC (2.8-fold, $P < 0.01$ vs. CH) or FAS (2.9-fold, $P < 0.001$ vs. CH, both not different vs. HFru-Veh). In keeping with the upregulated lipogenic enzymes, hepatic DNL was significantly increased (~38%) by PPARα activation in CH-fed mice, and this increase was maintained in HFru-FB mice (Fig. 6*E*). These data suggested the FB-induced UPR signaling may enhance the lipogenic capacity of liver independent of the effects of dietary fructose.

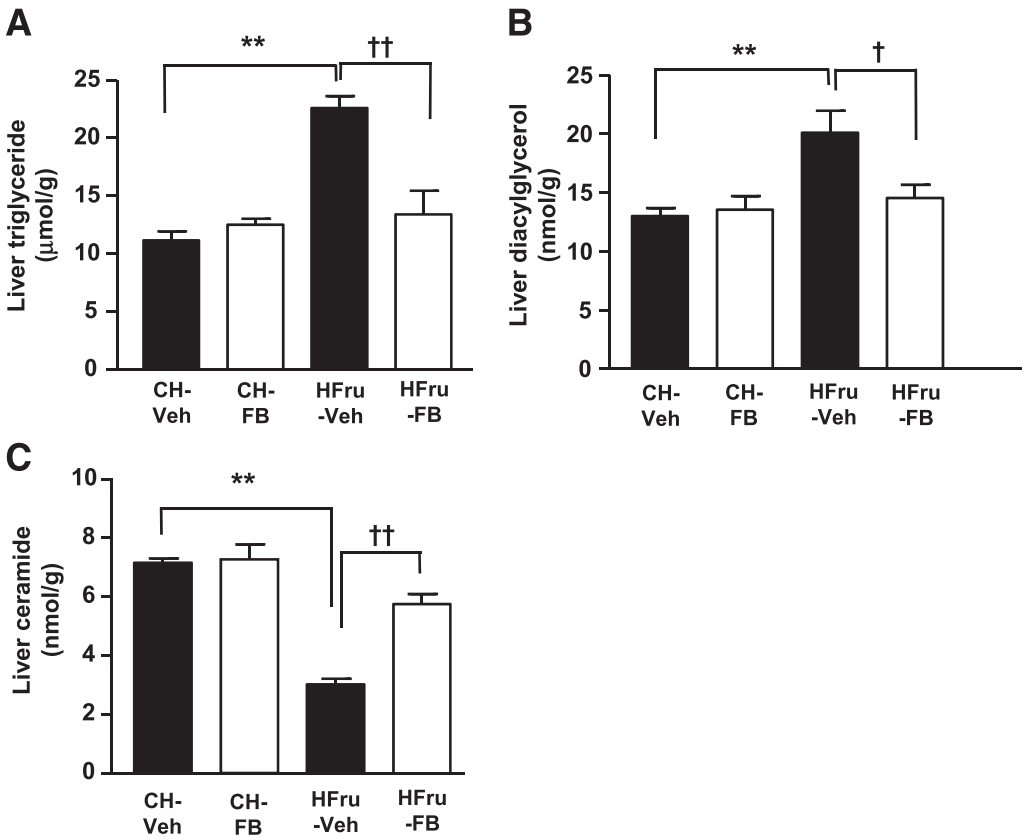

FIG. 3. Effects of FB treatment on hepatic lipid content. After 2 weeks of feeding, animals were fasted for 5–7 h before tissue collection, and liver homogenates were extracted for the assessment of total TG (*A*), DAG (*B*), and ceramide (*C*) content. Data are mean ± SE, 8 mice per group. **$P < 0.01$; †$P < 0.05$; ††$P < 0.001$ of the compared groups.

The downstream effects of the FB-induced UPR signaling. Production of deleterious lipids (lipotoxicity) through DNL and activation of serine/threonine kinases are key consequences of UPR signaling, which interferes with insulin signal transduction at various points (15). As shown in Fig. 3*B*, treatment with FB can correct the elevated DAG content induced by HFru feeding. Meanwhile, activation of JNK and IKK are well-demonstrated consequences of UPR signaling, resulting in the impairment of insulin signal transduction (3). HFru feeding did not result in a significant induction of JNK (Fig. 7*A*) or IKK (Fig. 7*B*), and the expression of IκBα (Fig. 7*C*), the downstream target of IKK (32), remained unaffected, which is consistent with our previous observation (16). Despite the significant induction of the two specific arms of UPR pathways, the phosphorylation status of these kinases remained unaffected in response to FB treatment (Fig. 7*A*–*C*). These data suggest that PPARα activation is effective in eliminating lipotoxicity and that the FB-induced UPR signaling did not result in the activation of these stress kinases.

DISCUSSION

The current study has established a hepatic ER stress model independent of lipid accumulation in the liver with the use of the PPARα activator FB in HFru-fed mice. This model enabled us to examine the effects of ER stress on hepatic insulin sensitivity devoid of the influence of hepatic steatosis. The data show that PPARα activation completely eliminated HFru-induced hepatic steatosis and insulin resistance without altering JNK and IKK in the face of marked dual activation of the IRE1/XBP1 and PERK/eIF2α branches of the UPR pathways. These findings indicate that hepatic steatosis, but not JNK, is required for ER stress to cause insulin resistance. To the best of our knowledge, this report is the first to demonstrate that PPARα activation induces UPR signaling while ameliorating hepatic insulin resistance.

PPARα is a key transcriptional regulator for lipid metabolism, and it can be endogenously activated by FAs as well as pharmacologically activated by agonists like FB (17). FB is a specific agonist of PPARα commonly used to treat dyslipidemia and hypercholesterolemia in humans (33). These beneficial effects are attributed to the PPARα-driven peroxisomal and mitochondrial β-oxidation and microsomal ω-oxidation of FA, with the liver being a major site of action (34). The data show that FB treatment was effective in activating PPARα in vivo as evidenced by the increased expression of ACOX1 (also known as palmitoyl-CoA oxidase) (35), which is a direct target of PPARα. The concomitant increase in V_{O_2} and the induction of the phosphorylated form of ACC and β-HAD activity along with the augmented FA oxidation in the liver are indicative of an enhanced oxidative capacity and energy expenditure, which are consistent with the reported effects of PPARα activation (34,36). In line with the upregulation of ACOX1 expression, FB-induced increase in hepatic FA oxidation can be attributed to the enhanced peroxisomal oxidation that is not inhabitable by etomoxir, which blocks the entry of long-chain FAs into mitochondria for oxidation. It has been reported that peroxisomal oxidation breakdown of (very) long-chain FAs into medium- and short-chain FAs

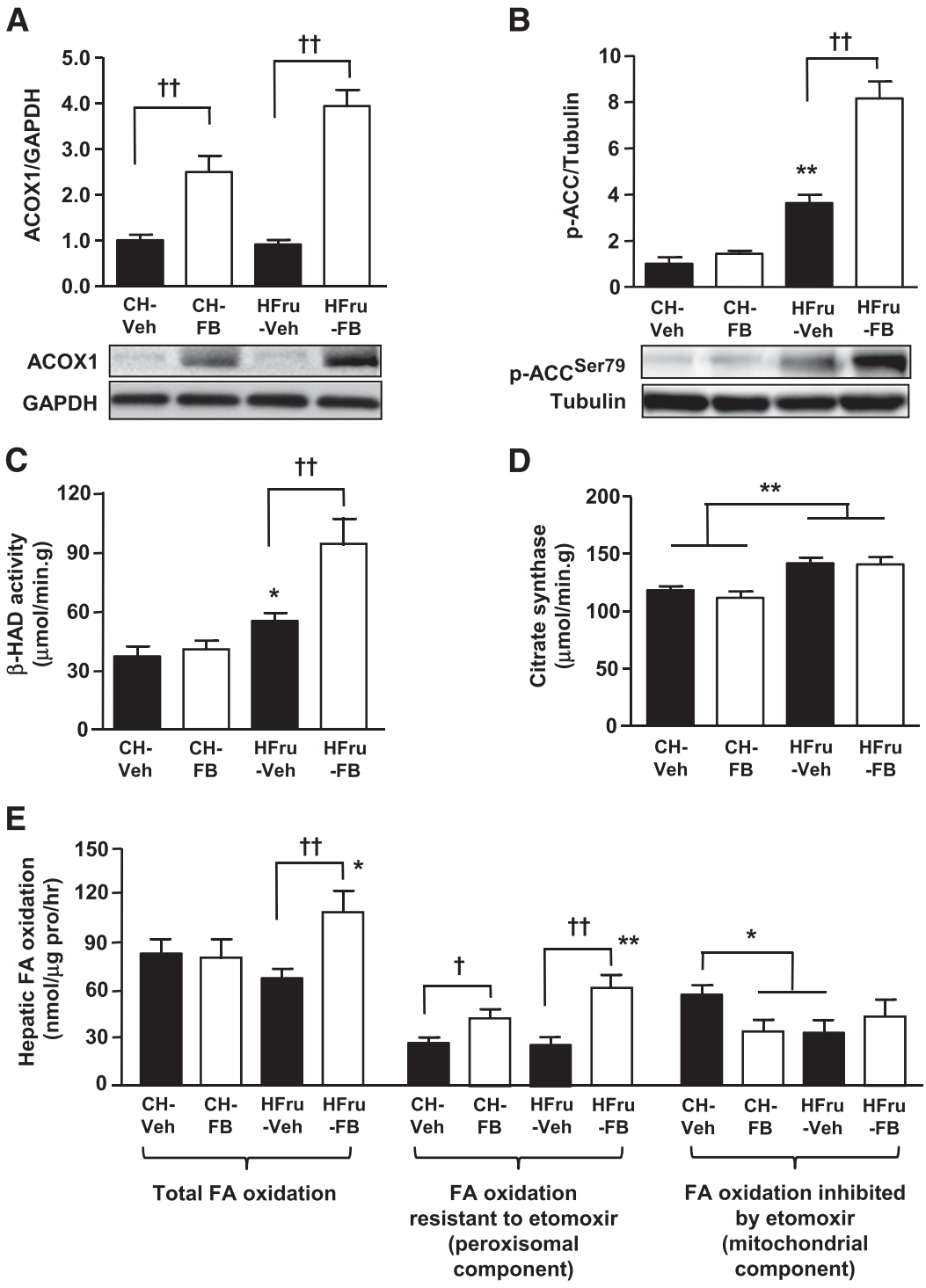

FIG. 4. Effects of FB treatment on key enzymes of FA oxidation. After 2 weeks of feeding, animals were fasted for 5–7 h before tissue collection, and liver homogenates were immunoblotted for key enzymes related to oxidative capacity. Representative blots of ACOX1 (*A*), phosphorylated (p) ACC (Ser79) (*B*), the specific activities of β-HAD (*C*), and citrate synthase (*D*). Each lane represents a single mouse. Data are mean ± SE, 10 mice per group. *E*: Hepatic FA oxidation was measured in separate liver homogenates with [^{14}C]palmitate as a substrate in the presence or absence of 0.02 mmol/L etomoxir. Data are mean ± SE, 6–8 mice per group. *$P < 0.05$; **$P < 0.01$ vs. CH; †$P < 0.05$; ††$P < 0.001$ of the compared groups.

further oxidation in mitochondria (36). Unlike long-chain FAs, the short- and medium-chain FAs do not rely on carnitine palmitoyltransferase 1 to enter the mitochondria (36), which may explain, at least in part, the increased oxygen consumption observed at the whole-body level. It is likely that the reduced body weight and adiposity observed only in HFru-FB mice is a result of enhanced peroxisomal oxidation, which was not evident in CH-FB mice.

The restored HOMA-IR resulting from the lowered fasting blood glucose and insulin levels together with the restored hepatic insulin signal transduction in the HFru-fed

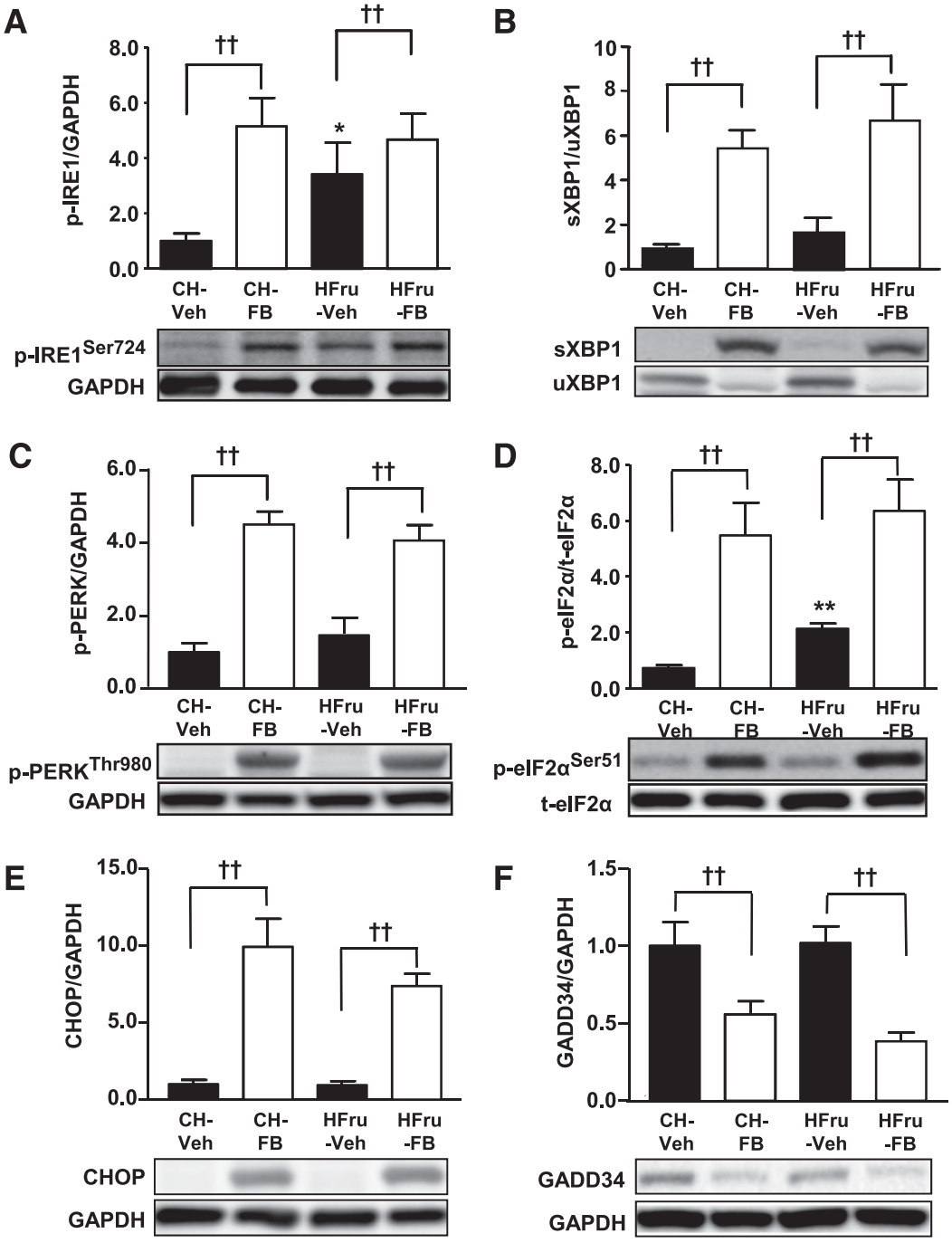

FIG. 5. Effects of FB treatment on hepatic UPR signaling. After 2 weeks of feeding, animals were fasted for 5–7 h before tissue collection, and liver homogenates were immunoblotted for markers of ER stress. Representative blots of phosphorylated (p) IRE1 (Ser724) (*A*), sXBP1 (*B*), p-PERK (Thr980) (*C*), p-eIF2α (Ser51) (*D*), CHOP (*E*), and GADD34 (*F*) with densitometry. Each lane represents a single mouse. Data are mean ± SE, 8–10 mice per group. *$P < 0.01$, $P < 0.01$ vs. CH; ††$P < 0.01$ of the compared groups.

mice by FB suggest improved insulin sensitivity in these mice. This interpretation is also supported by the striking reduction in insulin secretion in CH-FB mice while maintaining unaltered glucose clearance. The insulin-sensitizing effect of FB observed in the current study is consistent with our previous report of the insulin-sensitizing effect of PPARα activation in high fat–fed insulin resistant rats as determined by the hyperinsulinemic-euglycemic clamp (37).

The ER plays a pivotal role in protein processing to maintain cellular homeostasis under physiological conditions through the three canonical branches of UPR signaling pathways: PERK/eIF2α, IRE1/XBP1, and ATF6. The initialing proteins PERK, IRE, and ATF6 all have sensors facing the ER lumen, and they can be activated under ER stress, such as the accumulation of misfolded proteins (9,15). The activated IRE1/XBP1 pathway has been suggested to promote DNL in the liver, leading to the production of lipids (4,7). In addition, both IRE1 (10) and PERK (38) have been suggested to activate JNK and IKK. These mechanisms, acting in concert or alone, are sufficient to impair insulin signaling in the liver. However, it has been difficult to separate the effect of activated UPR

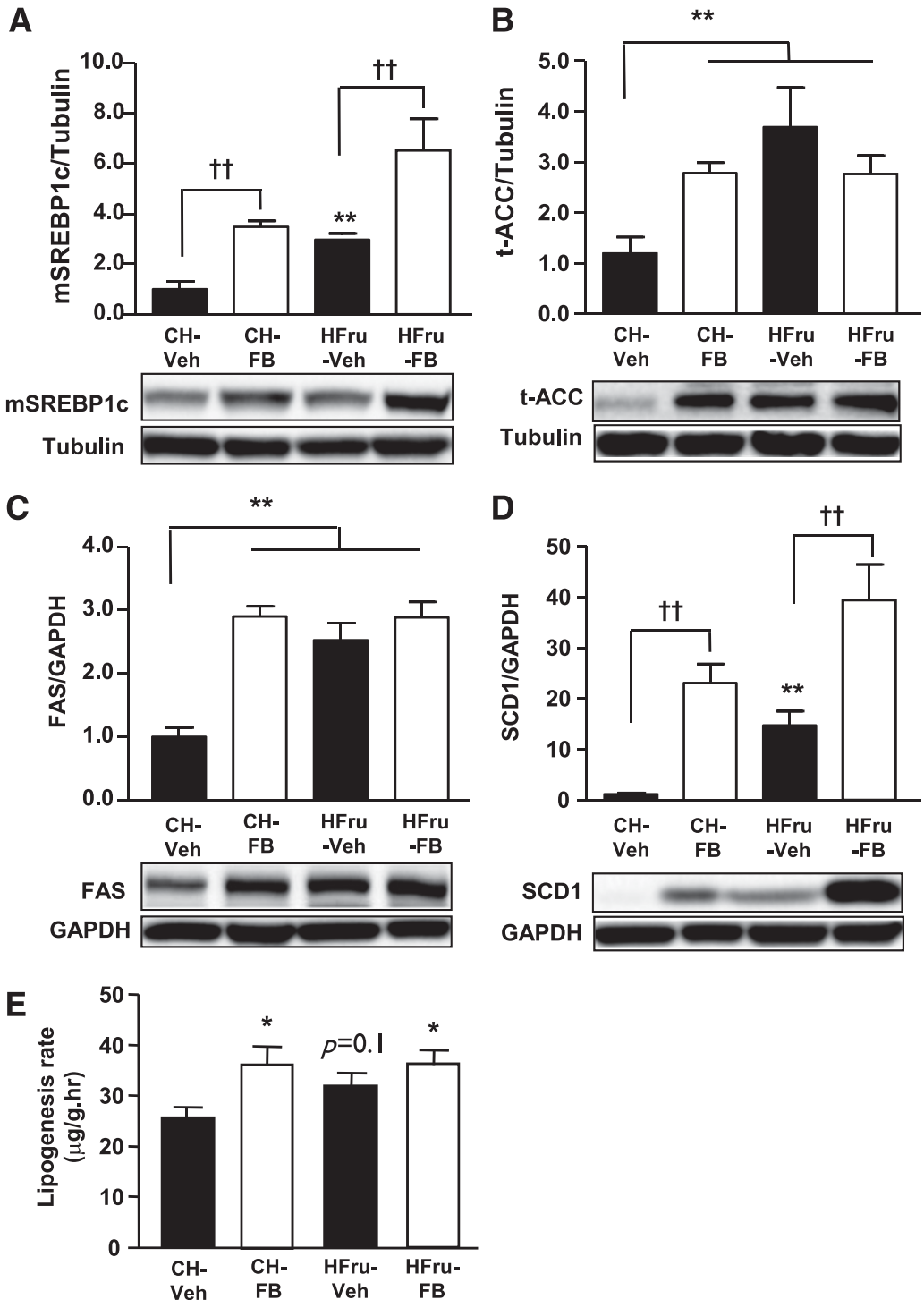

FIG. 6. Effects of FB treatment on hepatic DNL. After 2 weeks of feeding, animals were fasted for 5–7 h before tissue collection, and liver homogenates were immunoblotted for key enzymes related to lipogenic capacity. Representative blots of the mSREBP1c (*A*), total (t) ACC (*B*), FAS (*C*), and SCD1 (*D*) with densitometry. Data are mean ± SE, 10 mice per group. *E*: Hepatic DNL was measured by the incorporation of $[^3H]H_2O$ into hepatic TG. Data are mean ± SE, 6–8 mice per group. *$P < 0.05$; **$P < 0.01$ vs. CH; ††$P < 0.001$ of the compared groups.

pathways on hepatic insulin signaling in vivo from the influence of lipid accumulation. Moreover, FB is a lipid-lowering drug commonly used in humans, and fructose consumption is closely related to the epidemic of obesity and fatty liver (6,39). Thus, the approach of administration of FB to insulin resistant mice induced by HFru feeding would not only allow us to dissect such an integral relationship, but also to provide insight into the mechanism relevant to human conditions.

Both DAG and ceramide are key lipid intermediaries that link hepatic steatosis to insulin resistance (4). The results show that liver DAG content was higher in HFru-fed mice (as a result of increased DNL), and this is consistent with a previous report in HFru-fed mice (40). DAG

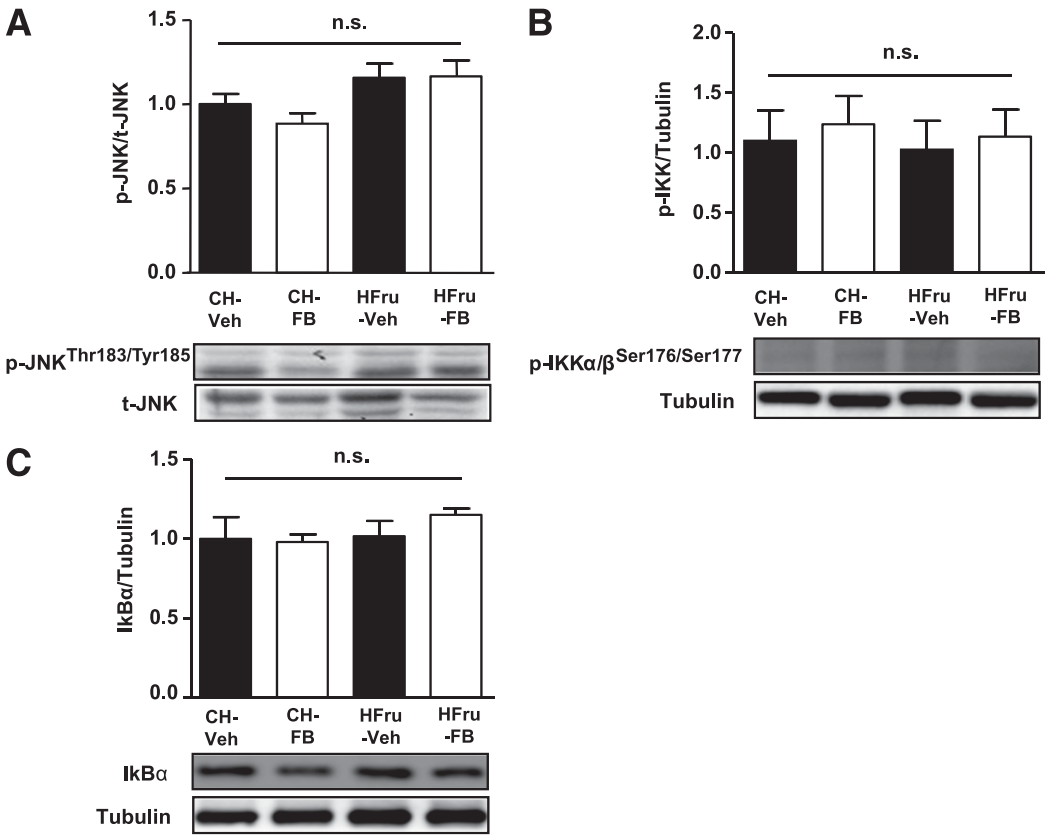

FIG. 7. Effects of FB treatment on JNK and IKK activation. After 2 weeks of feeding, animals were fasted for 5–7 h before tissue collection, and liver homogenates were immunoblotted for evidence of JNK and IKK activation. Representative blots of phosphorylated (p) JNK (Thr183/Tyr185) (*A*), p-IKKα/β (Ser176/Ser177) (*B*), and IκBα (*C*). Data are mean ± SE, 8 mice per group.

can activate protein kinases C ε, which in turn phosphorylates IRS1 at serine 307 to disrupt tyrosine phosphorylation of IRS1 (41). This could blunt IRS-mediated phosphorylation of its downstream signaling target, such as Akt (42). While maintaining elevated DNL (as indicated by mSREBP1c, ACC, FAS, and SCD1 and the incorporation of $[^3H]H_2O$ into TG) induced by an HFru diet, FB outpaced DNL by a much greater effect to accelerate FA oxidation (as indicated by the 14–16% increase in VO_2 and 3.9-fold, 8-fold, and 2.1-fold increases in ACOX1, p-ACC, and β-HAD, respectively), hence eliminating the accumulation of TG and DAG. This may offer an explanation for the improved insulin signaling by FB. In HFru-fed rat, hepatic ceramide has been reported to be increased (43), and this lipid metabolite can suppress the phosphorylation of Akt through protein phosphatase 2A (44,45). In the current study, ceramide is unlikely to be a contributor for the blunted insulin signaling because its level in HFru-FB mice was similar to the level in CH-fed mice. However, the precise role of ceramide requires further investigation because the cellular location may be a key determinant of its effect on insulin sensitivity (46).

The other key mechanism for ER stress-induced insulin resistance is the activation of JNK and associated stress kinases. Sustained ER stress has been shown to cause hepatic insulin resistance through the induction of JNK and IKK (8,13), and all three canonical arms of the UPR pathways are capable of activating JNK and IKK signaling under conditions of severe ER stress (3). Consistent with our previous finding (16), HFru feeding was accompanied by the presence of ER stress. Despite further activation of the IRE1/XBP1 and PERK/eIF2α signaling by the activation of PPARα with FB, the unaltered phosphorylation of JNK and IKK or IκBα content argues against their role in the improved insulin-signaling properties in the liver. In addition, cellular ceramide is known to be implicated in the upregulation of IKK and JNK (44). The fact that neither ceramide nor these stress-related kinases were upregulated by FB is also consistent with our interpretation of the reduction in DAGs as a more likely mechanism for the alleviation of hepatic insulin resistance by the activation of PPARα. Of interest, Jurczak et al. (40) recently demonstrated alleviation of hepatic DAG accumulation in mice with conditional knockout of XBP1. The absence of XBP1 can reverse fructose-induced insulin resistance despite the presence of ER stress and JNK activation, which supports the notion of DAGs being the major culprit for hepatic insulin resistance induced by HFru feeding.

It has been suggested that mild ER stress may enhance hepatic insulin signaling and protect against lipotoxicity through the induction of an adaptive UPR (47). Mice carrying liver-specific deletion of IRE1 showed overt steatosis when challenged with ER stress inducers (48), whereas genetic ablation of either ER stress-sensing or ER quality-control molecules also resulted in the development of hepatic steatosis (49). Furthermore, IRE1 has been reported to be capable of repressing the expression of key metabolic transcriptional regulators, including C/EBPβ, C/EBPδ, PPARγ, and enzymes involved in TG biosynthesis (49), suggesting that UPR might be an important mechanism for mitigating steatosis. The current study results highlight the need for further investigation to examine

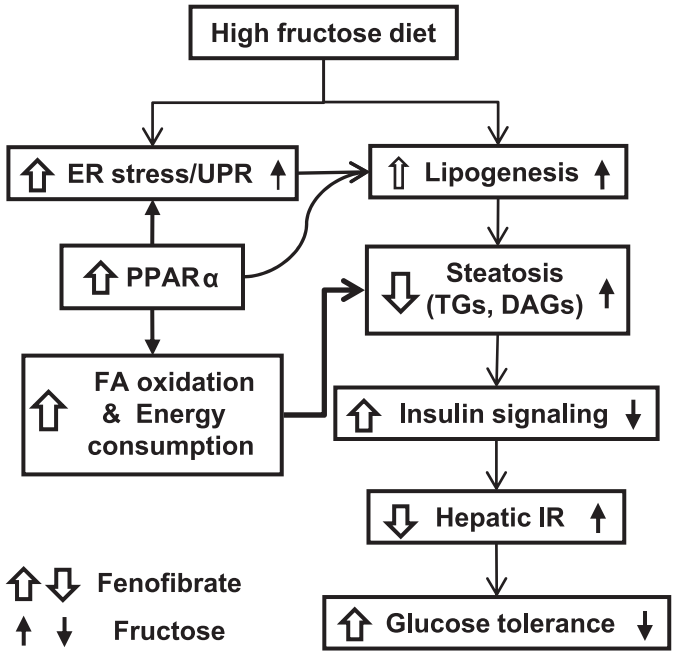

FIG. 8. Illustration of PPARα-mediated effects on ER stress, lipid metabolism, and insulin sensitivity in the liver. HFru feeding accentuates the accumulation of TG and DAG in the liver through the induction of DNL. The accumulation of these lipid metabolites attenuates normal insulin signal transduction leading to hepatic insulin resistance, resulting in the reduction of glucose tolerance. PPARα activation by FB may also directly stimulate lipogenesis, which may involve the signaling of specific arms of the UPR pathways. However, the predominant effect of potentiated oxidative capacity (primarily peroxisomal oxidation) driven by PPARα is capable of eliminating lipid accumulation, thus overcoming fructose-induced hepatic insulin resistance (IR) and glucose intolerance.

whether specific UPR signaling may in fact contribute to the PPARα-mediated effects on insulin sensitivity.

Although attenuated body weight gain in the HFru-fed mice induced by FB may cloud our interpretation at first glance, the pivotal role of lipids (but not the activated UPR per se) in ER stress–associated insulin resistance is also demonstrated in CH-FB mice without body weight change (compared with CH-fed mice). Despite similar dual activation of both IRE1/XBP1 and PERK/eIF2α pathways in the CH-FB mice, insulin-mediated phosphorylation of Akt and GSK3β remained intact in the absence of lipid accumulation. This interpretation is consistent with a previous study that showed reduced liver lipids as the underlying mechanism of improved hepatic insulin sensitivity during body weight loss in patients with type 2 diabetes (50).

In summary, the data indicate that lipid (particularly DAG) accumulation, but not the activation of JNK or IKK, is required for ER stress to cause hepatic insulin resistance and glucose intolerance during HFru consumption. Increased peroxisomal oxidation of FAs and energy expenditure are likely to underpin the observed reduction in hepatic steatosis and insulin resistance in HFru-FB mice despite marked increases in UPR signaling and DNL. Therefore, activation of PPARα with FB ameliorates HFru-induced hepatic insulin resistance by eliminating lipid deposition by blocking its link with the ER (Fig. 8). The findings also suggest a need for further investigation into whether activation of specific UPR pathways may in fact contribute to the therapeutic effects of fibrate drugs, which are commonly used in humans.

ACKNOWLEDGMENTS

This study was supported by the National Health and Medical Research Council of Australia Program Grant 535921 (allocation to J.-M.Y.) and Australian Research Council (DP 110102396 to J.-M.Y.). M.J.W. is a Senior Research Fellow of National Health and Medical Research Council.

No potential conflicts of interest relevant to this article were reported.

S.M.H.C. designed the study, contributed to the research data, and wrote the manuscript. R.-Q.S. contributed to the research data and wrote the manuscript. X.-Y.Z., Z.-H.C., and H.W. contributed to the research data. M.J.W. contributed to the research data and provided reagents, materials, and analysis tools. J.-M.Y. conceived and designed the study, provided reagents, materials, and analysis tools, and wrote the manuscript. J.-M.Y. is the guarantor of this work and, as such, had full access to all the data in the study and takes responsibility for the integrity of the data and accuracy of the data analysis.

The authors thank Dr. Juan Carlos Molero for his comments and Xiu Zhou and Songpei Li (RMIT University) for their technical assistance.

REFERENCES

1. Samuel VT, Shulman GI. Mechanisms for insulin resistance: common threads and missing links. Cell 2012;148:852–871
2. Rizza RA. Pathogenesis of fasting and postprandial hyperglycemia in type 2 diabetes: implications for therapy. Diabetes 2010;59:2697–2707
3. Hotamisligil GS. Endoplasmic reticulum stress and the inflammatory basis of metabolic disease. Cell 2010;140:900–917
4. Samuel VT, Petersen KF, Shulman GI. Lipid-induced insulin resistance: unravelling the mechanism. Lancet 2010;375:2267–2277
5. Stanhope KL, Schwarz JM, Keim NL, et al. Consuming fructose-sweetened, not glucose-sweetened, beverages increases visceral adiposity and lipids and decreases insulin sensitivity in overweight/obese humans. J Clin Invest 2009;119:1322–1334
6. Maersk M, Belza A, Stødkilde-Jørgensen H, et al. Sucrose-sweetened beverages increase fat storage in the liver, muscle, and visceral fat depot: a 6-mo randomized intervention study. Am J Clin Nutr 2012;95:283–289
7. Lee AH, Scapa EF, Cohen DE, Glimcher LH. Regulation of hepatic lipogenesis by the transcription factor XBP1. Science 2008;320:1492–1496
8. Ozcan U, Yilmaz E, Ozcan L, et al. Chemical chaperones reduce ER stress and restore glucose homeostasis in a mouse model of type 2 diabetes. Science 2006;313:1137–1140
9. Ron D, Walter P. Signal integration in the endoplasmic reticulum unfolded protein response. Nat Rev Mol Cell Biol 2007;8:519–529
10. Urano F, Wang X, Bertolotti A, et al. Coupling of stress in the ER to activation of JNK protein kinases by transmembrane protein kinase IRE1. Science 2000;287:664–666
11. Hu P, Han Z, Couvillon AD, Kaufman RJ, Exton JH. Autocrine tumor necrosis factor alpha links endoplasmic reticulum stress to the membrane death receptor pathway through IRE1alpha-mediated NF-kappaB activation and down-regulation of TRAF2 expression. Mol Cell Biol 2006;26:3071–3084
12. Liang SH, Zhang W, McGrath BC, Zhang P, Cavener DR. PERK (eIF2alpha kinase) is required to activate the stress-activated MAPKs and induce the expression of immediate-early genes upon disruption of ER calcium homoeostasis. Biochem J 2006;393:201–209
13. Ozcan U, Cao Q, Yilmaz E, et al. Endoplasmic reticulum stress links obesity, insulin action, and type 2 diabetes. Science 2004;306:457–461
14. Gao Z, Hwang D, Bataille F, et al. Serine phosphorylation of insulin receptor substrate 1 by inhibitor kappa B kinase complex. J Biol Chem 2002;277:48115–48121
15. Fu S, Watkins SM, Hotamisligil GS. The role of endoplasmic reticulum in hepatic lipid homeostasis and stress signaling. Cell Metab 2012;15:623–634
16. Ren LP, Chan SM, Zeng XY, et al. Differing endoplasmic reticulum stress response to excess lipogenesis versus lipid oversupply in relation to hepatic steatosis and insulin resistance. PLoS ONE 2012;7:e30816
17. Chakravarthy MV, Lodhi IJ, Yin L, et al. Identification of a physiologically relevant endogenous ligand for PPARalpha in liver. Cell 2009;138:476–488

18. Oosterveer MH, Grefhorst A, van Dijk TH, et al. Fenofibrate simultaneously induces hepatic fatty acid oxidation, synthesis, and elongation in mice. J Biol Chem 2009;284:34036–34044
19. Lalloyer F, Wouters K, Baron M, et al. Peroxisome proliferator-activated receptor-alpha gene level differently affects lipid metabolism and inflammation in apolipoprotein E2 knock-in mice. Arterioscler Thromb Vasc Biol 2011;31:1573–1579
20. Anderlová K, Dolezalová R, Housová J, et al. Influence of PPAR-alpha agonist fenofibrate on insulin sensitivity and selected adipose tissue-derived hormones in obese women with type 2 diabetes. Physiol Res 2007;56:579–586
21. Molero JC, Waring SG, Cooper A, et al. Casitas b-lineage lymphoma-deficient mice are protected against high-fat diet-induced obesity and insulin resistance. Diabetes 2006;55:708–715
22. Tan MJ, Ye JM, Turner N, et al. Antidiabetic activities of triterpenoids isolated from bitter melon associated with activation of the AMPK pathway. Chem Biol 2008;15:263–273
23. Turner N, Bruce CR, Beale SM, et al. Excess lipid availability increases mitochondrial fatty acid oxidative capacity in muscle: evidence against a role for reduced fatty acid oxidation in lipid-induced insulin resistance in rodents. Diabetes 2007;56:2085–2092
24. Weis BC, Cowan AT, Brown N, Foster DW, McGarry JD. Use of a selective inhibitor of liver carnitine palmitoyltransferase I (CPT I) allows quantification of its contribution to total CPT I activity in rat heart. Evidence that the dominant cardiac CPT I isoform is identical to the skeletal muscle enzyme. J Biol Chem 1994;269:26443–26448
25. Dietschy JM, Spady DK. Measurement of rates of cholesterol synthesis using tritiated water. J Lipid Res 1984;25:1469–1476
26. Preiss J, Loomis CR, Bishop WR, Stein R, Niedel JE, Bell RM. Quantitative measurement of sn-1,2-diacylglycerols present in platelets, hepatocytes, and ras- and sis-transformed normal rat kidney cells. J Biol Chem 1986;261:8597–8600
27. Kersten S, Seydoux J, Peters JM, Gonzalez FJ, Desvergne B, Wahli W. Peroxisome proliferator-activated receptor alpha mediates the adaptive response to fasting. J Clin Invest 1999;103:1489–1498
28. Leone TC, Weinheimer CJ, Kelly DP. A critical role for the peroxisome proliferator-activated receptor alpha (PPARalpha) in the cellular fasting response: the PPARalpha-null mouse as a model of fatty acid oxidation disorders. Proc Natl Acad Sci U S A 1999;96:7473–7478
29. Inagaki T, Dutchak P, Zhao G, et al. Endocrine regulation of the fasting response by PPARalpha-mediated induction of fibroblast growth factor 21. Cell Metab 2007;5:415–425
30. Dreyer C, Krey G, Keller H, Givel F, Helftenbein G, Wahli W. Control of the peroxisomal beta-oxidation pathway by a novel family of nuclear hormone receptors. Cell 1992;68:879–887
31. Kammoun HL, Chabanon H, Hainault I, et al. GRP78 expression inhibits insulin and ER stress-induced SREBP-1c activation and reduces hepatic steatosis in mice. J Clin Invest 2009;119:1201–1215
32. Arkan MC, Hevener AL, Greten FR, et al. IKK-beta links inflammation to obesity-induced insulin resistance. Nat Med 2005;11:191–198
33. Keating GM. Fenofibrate: a review of its lipid-modifying effects in dyslipidemia and its vascular effects in type 2 diabetes mellitus. Am J Cardiovasc Drugs 2011;11:227–247
34. Reddy JK, Goel SK, Nemali MR, et al. Transcription regulation of peroxisomal fatty acyl-CoA oxidase and enoyl-CoA hydratase/3-hydroxyacyl-CoA dehydrogenase in rat liver by peroxisome proliferators. Proc Natl Acad Sci U S A 1986;83:1747–1751
35. Wanders RJ, Waterham HR. Biochemistry of mammalian peroxisomes revisited. Annu Rev Biochem 2006;75:295–332
36. Reddy JK, Rao MS. Lipid metabolism and liver inflammation. II. Fatty liver disease and fatty acid oxidation. Am J Physiol Gastrointest Liver Physiol 2006;290:G852–G858
37. Ye JM, Doyle PJ, Iglesias MA, Watson DG, Cooney GJ, Kraegen EW. Peroxisome proliferator-activated receptor (PPAR)-alpha activation lowers muscle lipids and improves insulin sensitivity in high fat-fed rats: comparison with PPAR-gamma activation. Diabetes 2001;50:411–417
38. Timmins JM, Ozcan L, Seimon TA, et al. Calcium/calmodulin-dependent protein kinase II links ER stress with Fas and mitochondrial apoptosis pathways. J Clin Invest 2009;119:2925–2941
39. Stanhope KL. Role of fructose-containing sugars in the epidemics of obesity and metabolic syndrome. Annu Rev Med 2012;63:329–343
40. Jurczak MJ, Lee AH, Jornayvaz FR, et al. Dissociation of inositol-requiring enzyme (IRE1α)-mediated c-Jun N-terminal kinase activation from hepatic insulin resistance in conditional X-box-binding protein-1 (XBP1) knock-out mice. J Biol Chem 2012;287:2558–2567
41. Yu C, Chen Y, Cline GW, et al. Mechanism by which fatty acids inhibit insulin activation of insulin receptor substrate-1 (IRS-1)-associated phosphatidylinositol 3-kinase activity in muscle. J Biol Chem 2002;277:50230–50236
42. Neschen S, Morino K, Hammond LE, et al. Prevention of hepatic steatosis and hepatic insulin resistance in mitochondrial acyl-CoA:glycerol-sn-3-phosphate acyltransferase 1 knockout mice. Cell Metab 2005;2:55–65
43. Vilà L, Roglans N, Alegret M, Sánchez RM, Vázquez-Carrera M, Laguna JC. Suppressor of cytokine signaling-3 (SOCS-3) and a deficit of serine/threonine (Ser/Thr) phosphoproteins involved in leptin transduction mediate the effect of fructose on rat liver lipid metabolism. Hepatology 2008;48:1506–1516
44. Chavez JA, Summers SA. A ceramide-centric view of insulin resistance. Cell Metab 2012;15:585–594
45. Schmitz-Peiffer C, Craig DL, Biden TJ. Ceramide generation is sufficient to account for the inhibition of the insulin-stimulated PKB pathway in C2C12 skeletal muscle cells pretreated with palmitate. J Biol Chem 1999;274:24202–24210
46. Bruce CR, Hoy AJ, Turner N, et al. Overexpression of carnitine palmitoyltransferase-1 in skeletal muscle is sufficient to enhance fatty acid oxidation and improve high-fat diet-induced insulin resistance. Diabetes 2009;58:550–558
47. Achard CS, Laybutt DR. Lipid-induced endoplasmic reticulum stress in liver cells results in two distinct outcomes: adaptation with enhanced insulin signaling or insulin resistance. Endocrinology 2012;153:2164–2177
48. Zhang K, Wang S, Malhotra J, et al. The unfolded protein response transducer IRE1α prevents ER stress-induced hepatic steatosis. EMBO J 2011;30:1357–1375
49. Rutkowski DT, Wu J, Back SH, et al. UPR pathways combine to prevent hepatic steatosis caused by ER stress-mediated suppression of transcriptional master regulators. Dev Cell 2008;15:829–840
50. Petersen KF, Dufour S, Befroy D, Lehrke M, Hendler RE, Shulman GI. Reversal of nonalcoholic hepatic steatosis, hepatic insulin resistance, and hyperglycemia by moderate weight reduction in patients with type 2 diabetes. Diabetes 2005;54:603–608